Structural Durability & Health Monitoring
DOI:10.32604/sdhm.2020.09104
Article

Long-Term Bending Behaviour of Prestressed Glulam Bamboo-Wood Beam Based on Creep Effect

Nan Guo[1,*], Huajing Xiong[1], Mingtao Wu[1], Hongliang Zuo[1], Fengguo Jiang[2], Xiaofeng Hou[3] and Dabo Xin[1]

[1]School of Civil Engineering, Northeast Forestry University, Harbin, 150040, China
[2]School of Civil Engineering, Heilongjiang University of Science and Technology, Harbin, 150027, China
[3]Heilongjiang Metallurgical Design Planning Institute, Harbin, 150040, China
*Corresponding Author: Nan Guo. Email: snowguonan@163.com
Received: 12 November 2019; Accepted: 03 March 2020

Abstract: Creep is an important characteristic of bamboo and wood materials under long-term loading. This paper aims to study the long-term bending behaviour of prestressed glulam bamboo-wood beam (GBWB). For this, 14 pre-stressed GBWBs were selected and subjected to a long-term loading test for 60 days. Then, a comparative analysis was performed for the effects of pre-tension values, the number of pre-stressed wires, and long-term load on the stress variation of the steel wire and the long-term deflection of the beam midspan. The test results showed that with the number of prestressed wires increasing, the total stress of the steel wire in the beam midspan and the ratio of the long-term deflection to the total deflection decreases decreased, but when the number of steel wires exceeded 4, the total stress and long-term deflection was less influenced; with the pre-tension value increasing, the ratio of the total stress of the steel wire in the beam midspan and the ratio of the long-term deflection to the total deflection also decreased, but when the prestress force was greater than 3.975 kN, the total stress and long-term deflection were less affected; with the other parameters unchanged, when the value of the long-term load increased, the total stress of the steel wire decreased, and the long-term deflection of the beam midspan increased, which shall be more significant with the long-term load greater than 30% of the standard ultimate bearing capacity. After the test, the experimental data were fitted, and the creep coefficient was given. Finally, the long-term stiffness calculation formula of the pre-stressed GBWB based on creep effect was proposed. The research findings have certain theoretical significance and engineering value.

Keywords: Prestressed glulam bamboo-wood beam; long-term loading test; steel wire stress; long-term deflection; creep coefficient

1 Introduction

Bamboo and wood construction have the advantages of energy-conservation and environment protection, safety and reliability, short cycle, renewability of materials, light weight and high strength. It is a popular and highly promising architectural form [1–9]. Bamboo-wood composites are formed by gluing bamboo and wood together, using high-strength bamboo for the component surface, and the wood easily processed inside the components, which fully utilize the advantages of these two materials [10–12]. When the traditional bamboo and wood beams are bent, the compressive strength of the material cannot be fully exerted in the failure mode of brittle tensile damage, and there is also a large deformation [13–18]. One research team proposed a new type of composite component-the prestressed glulam bamboo-wood beam, and also conducted the experimental study on the material selection and short-term bending behaviour of the beam [19–24]. It is well known that creep is a basic property of bamboo and wood materials, and has a great influence on the stress and deformation performance of bamboo and wood members [25]. Therefore, it is necessary to study the long-term bending behaviour of PGBGB, obtain the influence law of the creep on the stress degradation of the steel wire and the increase of the deflection in the beam span, and further clarify the long-term mechanical performance of such members, which has certain theoretical significance and engineering value.

At present, the research on creep at home and abroad mainly involves three parts: materials, components, and structures [26]. In [27], the stretching and compressing creep test was carried out on a new type of glulam bamboo material specimens under different stress levels for one year, to conclude the creep deformation law of such material. NurYazdani et al. studied the Burger model by the creep test on 16 simply supported beams for 895-day loading and 90 days off-loading, and then verified the applicability of the Burger model in simulating bending deformation [28]. The literature [29] carried out the long-term test and post-creep static failure test of the full-length glued bamboo beam bridge, and obtained its strength, stiffness and durability indexes, which provides a reference for the design of the bamboo structure bridge.

In this paper, a total of 14 pre-stressed GBWB were tested for a long period of 60 days to obtain the variation rule of steel wire stress and midspan deflection with time. Based on this, the influence of pre-tension value, pre-stressed wire quantity and long-term load on the long-term bending behaviour of the beam was summarized, and the creep coefficient characterizing its long-term deflection growth was put forward. Finally, the author proposed the long-term stiffness calculation formula of the pre-stressed GBWB.

2 Test Overview

2.1 Specimen Design and Grouping

The pre-stressed GBWB used in this test consists of bamboo-wood composites and prestressed tendons. The cross-section of bamboo-wood composite was 3,150 mm × 80 mm × 100 mm, made up of 3 layers of reconstituted bamboo boards and 2 layers of poplar, with the thickness of the laminate 20 mm, as shown in Fig. 1; the prestressed tendons were made of Grade 1570 low-relaxation prestressed round wires with a diameter of 7 mm. According to the number of steel wires, the value of prestress and the value of long-term load, the beams were classified into three groups: A, B and C. A group was used to research the influence of flexural property of beams that the number of steel wires caused, therefore its loading value rate and pretension value were not changed, and the number of steel wires was variable; B group was used to research the influence of flexural property of beams that the prestress value cause, so its number of steel wires and loading value rate were not altered, the pretension value is variable; the impact of long-term loading value on flexural property of beams was researched in C group, hence its number of steel wires and pretension value were not changed, the loading value rate was changed. The beam number can be written in the form of Lxm-n, where X represents the grouping of beams. N represents two beams in each working condition. Working condition is represented by m, but m represents different meanings in different groups respectively, in A group, m represents three different amounts of steel wires;in B group, m represents three different values of total pretension; in C group, m represents three different loading values (Tab. 1).

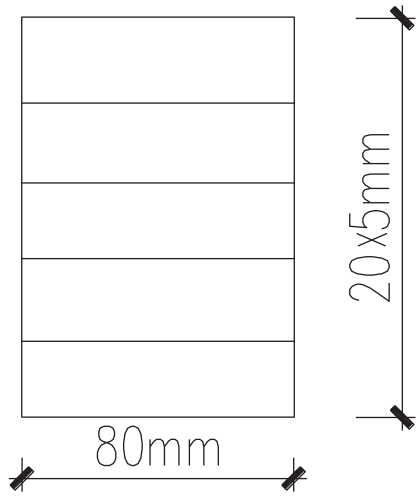

Figure 1: Cross section

Table 1: Basic information of test components

Beam group	Beam No.	Number of prestressed wires	Total pre-tension (kN)	Load value (kN)
A	L_{A1-1}	2	3.975	5.71
	L_{A1-2}	2	3.975	5.71
	L_{A2-1}	4	3.975	9.64
	L_{A2-2}	4	3.975	9.64
	L_{A3-1}	6	3.975	10.43
	L_{A3-2}	6	3.975	10.43
B	L_{B1-1}	4	1.987	7.14
	L_{B1-2}	4	1.987	7.14
	L_{B2-1}	4	3.975	9.64
	L_{B2-2}	4	3.975	9.64
	L_{B3-1}	4	5.962	10.31
	L_{B3-2}	4	5.962	10.31
C	L_{C1-1}	2	3.975	3.81
	L_{C1-2}	2	3.975	3.81
	L_{C2-1}	2	3.975	5.71
	L_{C2-2}	2	3.975	5.71
	L_{C3-1}	2	3.975	7.61
	L_{C3-2}	2	3.975	7.61

Note: The beam LA2-1 and LB2-1, beam LA2-2 and LB2-2, beam LA1-1 and LC2-1, beam LA1-2 and LC2-2 are identical respectively. They're numbered differently for different test purposes.

2.2 Loading Device and Measuring Point Arrangement

The long-term loading device used in this test was the same as the literature [30,31], as shown in Fig. 2, including one weight, one tray and two steel cables, as shown in Fig. 3. Weight actored the long-term loading, and it and beam were connected by cables and the trya. It has the characteristics of high bearing capacity, high rigidity, high efficiency and good applicability so that it could not only carry out long-term tests on 5 beams simultaneously, but also adjust the distance between the supports according to the length of the test beam, fully satisfying the requirements of the test.

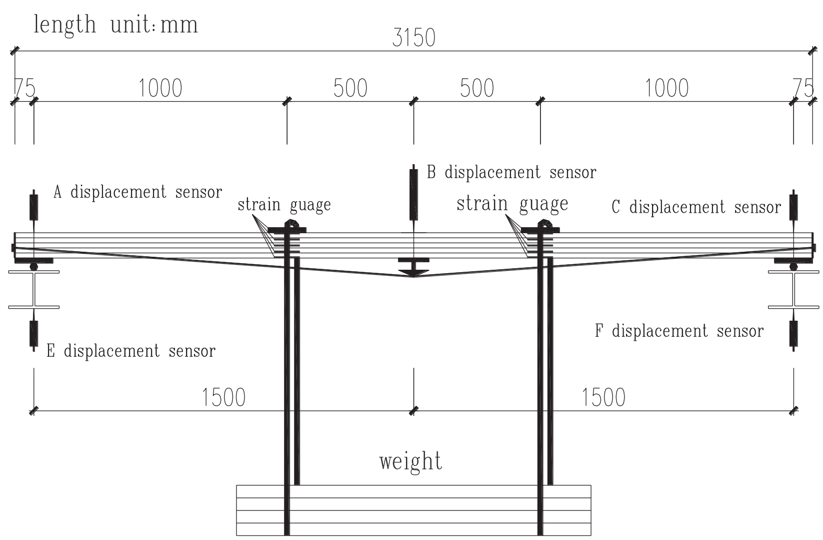

Figure 2: Long-term test loading

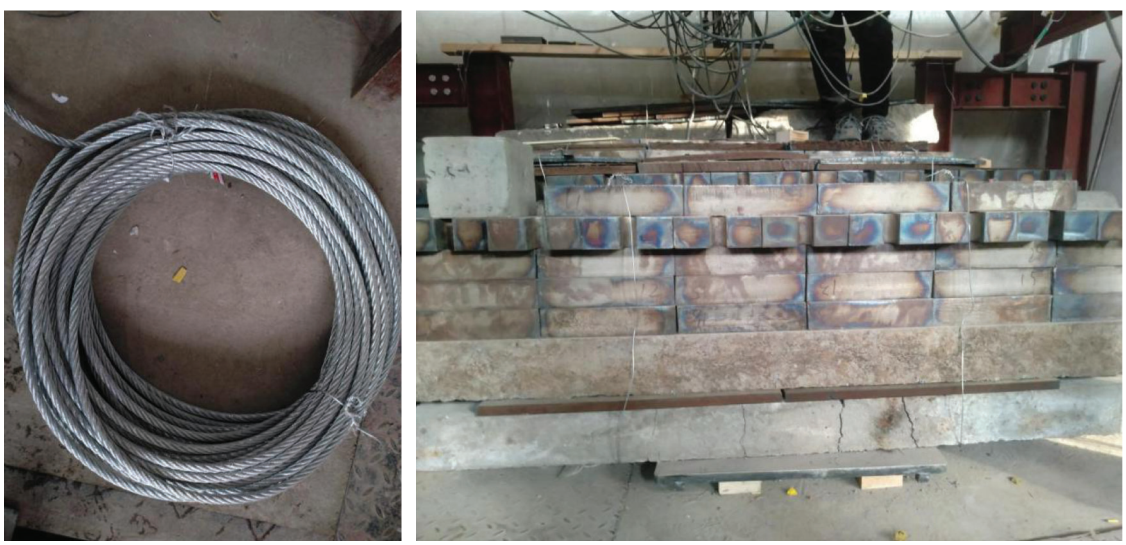

(a) (b)

Figure 3: Long-term test loading. (a) Steel cable and (b) Weight and tray

Based on the relationship between the load effect and the structural resistance, the inverse method [27] was used to concluding that the normal load on the pre-stressed GBWB was about 30% of the ultimate bearing capacity standard value of the beam, so as to determine the loading value of the test beam, as shown in Tab. 1.

The inverse method is concluded through normal standard calculation, therefore it can be introduced as follows, the magnitude of external loads has a relatively great impact on the creep development of glulam, which in turn affects the long-term deformation of the beam. This experiment aims to explore the influence of number of prestressed wires and total pre-tensions on the long-term flexural behavior of prestressed glulam beam string structures under normal use conditions. Therefore, a reasonable external load must be determined. According to the literature [32] and Load Code for the Design of Building Structures (GB50009-2012) [33], the relevant content of the derivation process of the bearing capacity design value of flexural members and load effect combinations is described. In terms of bearing capacity, the average value of the ultimate bearing capacity of the beam is first obtained from the short-term flexural test of prestressed glulam beam string structures. Then, the standard value of the ultimate bearing capacity is obtained based on the probability distribution and reliability requirements, and the design value is obtained through partial factors. In terms of load effects, prestressed members should use standard combinations under limit states of normal use, and basic combinations under limit states of bearing capacity. Let the load effect of the basic combination of prestressed glulam beam string structures be not greater than the bearing capacity, and according to the numerical relationship between the basic and standard combinations, the load value in the long-term test of prestressed glulam beam string structures can be derived. The detailed derivation process is shown in Fig. 4.

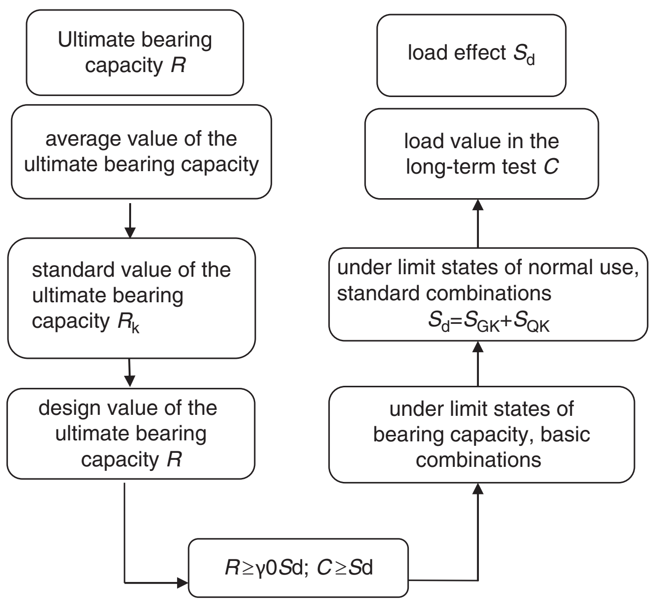

Figure 4: The derivation flowchart of the load value in the long-term loading test

The specific derivation process is as follows:

(1) Calculate the standard value Rk of the ultimate bearing capacity of prestressed glulam beam string structures.

According to the short-term loading test of prestressed glulam beam string structures, the test values of the ultimate bearing capacity for this test are μ_{R1}, μ_{R2}, μ_{R3}. Based on this, the average ultimate bearing capacity μ_R, standard deviation σ_R, and coefficient of variation V_R of the test beam can be obtained. The calculation of the above data can refer to formulas (1)–(3).

Average formula:

$$\bar{x} = \frac{1}{n}\sum_{i=1}^{n} x_i \tag{1}$$

Mean square deviation formula:

$$s = \sqrt{\frac{1}{n-1}\sum_{i=1}^{n}(x_i - \bar{x})^2} \tag{2}$$

Coefficient of variation formula:

$$C_v = s/|\bar{x}| \tag{3}$$

After the above data are calculated, the standard value of the ultimate bearing capacity of the beam can be obtained based on the formula (4):

$$R_k = \mu_R(1 - \alpha_R V_R) \tag{4}$$

where $\alpha_R = 1.645$ represents the quantile value with a certain guarantee rate.

(2) Calculate the design value R of the ultimate bearing capacity of prestressed glulam beam string structures.

$$R = R_k/\gamma_R \tag{5}$$

$$\gamma_R = (1 - \alpha_R V_R)/[1 - \beta(V_R\sigma_R/\sigma_Z)] \tag{6}$$

where γ_R represents the partial factor for resistance, which is usually 1.6 for the parallel-to-grain flexural wood structural members;

where β represents the reliability index, $\boldsymbol{\beta = (\mu_R - \mu_S)/\sigma_Z, \sigma_Z = (\sigma_R^2 + \sigma_S^2)^{0.5}}$; μ_R represents the mean value of resistance; μS represents the mean value of load effects.

(3) Calculate the load effect combination of prestressed glulam beam string structures under limit states of bearing capacity.

Prestressed glulam beam string structures should be calculated based on the basic combinations under limit states of bearing capacity. According to the literature [32], the effect ratio of variable load to permanent load of superstructures and office buildings can be 1.5. Assuming the standard value of the permanent load is G, then the standard value of the variable load is 1.5G, hence:

$$S_d = 1.2G + 1.4(1.5G) \tag{7}$$

(4) Calculate the load effect combination of prestressed glulam beam string structures under limit states of normal use.

Prestressed glulam beam string structures should be calculated based on the standard combinations under limit states of normal use. The variable load and permanent load in the formula (7) are substituted into the formulas (2)–(8) to obtain the standard load value of the beam in normal use.

$$S_d = G + 0.5(1.5G) \tag{8}$$

According to the formula (8), the standard load value of the beam in normal use is 0.33 times the standard value of its ultimate bearing capacity.

Based on the above derivation process and previous experimental experience, the load value of the long-term loading test of prestressed glulam beam string structures is determinated. Therefore above 30% of the standard value of ultimate bearing capacity was obtained from the short-term loading test of the beam.

According to relevant literature [34] and previous experimental experience, the loading time of this long-term test was set to be 60 days. In order to ensure a constant loading during the test, a three-point lifting method was used to apply long-term load, and steel backing plate and wooden block were placed at the three-point position to prevent local pressure damage [22] at the loading point, as shown in Fig. 5.

Figure 5: Picture of Long-term test loading

Three displacement meters were placed at the support and the mid-span position at both ends of the beam, in order to accurately measure the mid-span displacement of the beam; five strain gauges were evenly arranged along the beam height at two three-point locations of the beam, and two strain gauges were arranged across the top surface of the midspan, to obtain the stress distribution and variation in the bamboo-wood composite; a strain gauge was installed in the middle of each steel wire in order to obtain the stress variation of the steel wire. The positions of the displacement meters and the strain gauges are shown in Fig. 2.

When prestressing, the JM3813 model multi-function static strain test system was used to synchronize the data monitoring. After reaching the pre-tension value in Tab. 1, the stress value of the prestressed wire and that on each surface of the beam three-point were recorded, and then the loading started with the heavy objects hung on the beam. During the loading and holding process, the test data and the temperature and humidity in the surrounding environment were monitored in real time, and the interference of these factors on the laboratory was minimized.

3 Test Results and Analysis

3.1 Test Phenomenon

In order to compare and record the test phenomenon of the beam during long-term loading, the test beam was observed, photographed and recorded every 20 days, as shown in Fig. 6.

Fig. 6 shows that since the service load was applied, there appeared no cracks or similar phenomena on the pre-stressed GBWB during the whole long-term loading process, indicating that the test beam has been in a state of stable changes throughout the test.

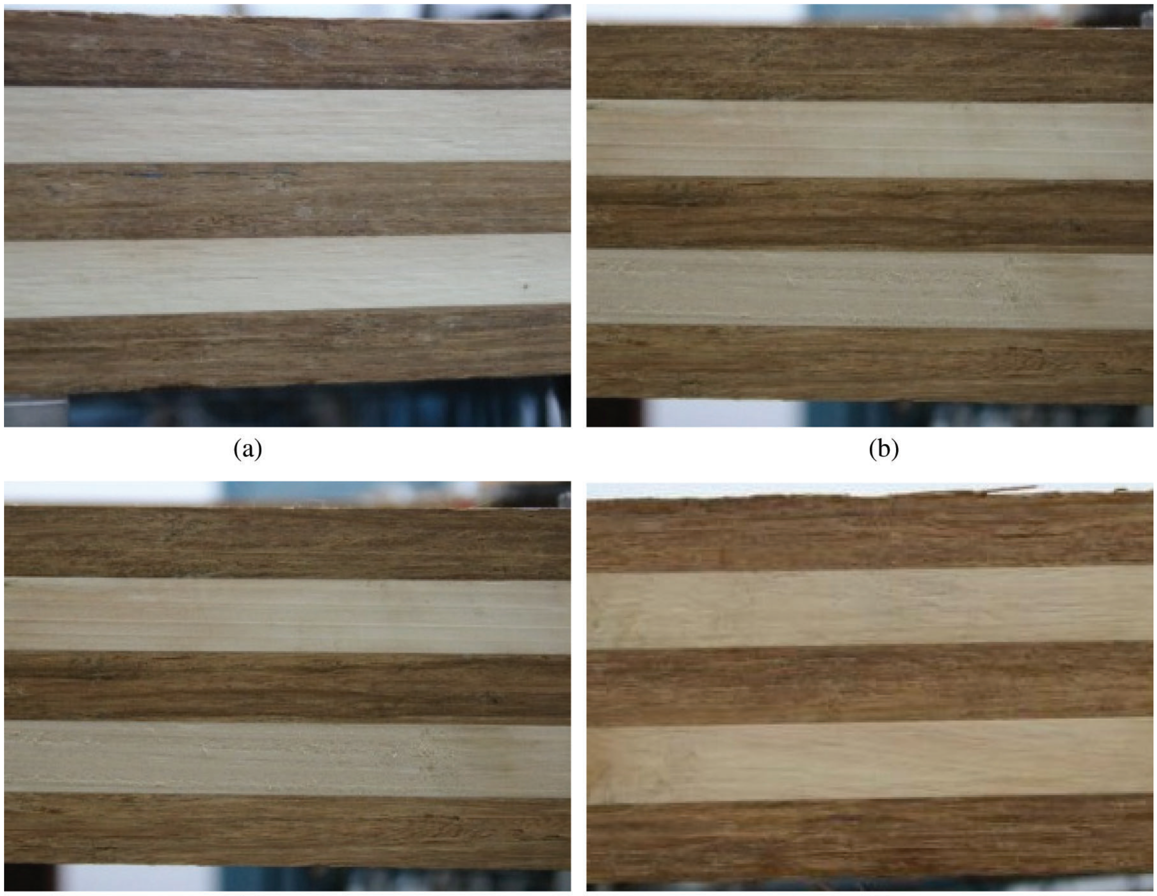

(a) (b)

(c) (d)

Figure 6: State diagram of pre-stressed GBWB during long-term test. (a) Test start, (b) The 20th day, (c) The 40th day and (d) The 60th day

3.2 Change Law of Prestressed Wire Stress

Because the initial stress of the prestressed wire was less than 0.5 times the ultimate tensile strength R_y, the relaxation phenomenon of the steel wire was not obvious, which can be ignored in this test [9]. Then, it can be considered that the changes of steel wire stress are entirely caused by the creep of the bamboo-wood composite.

Fig. 7 shows the curves of total wire stress with time for the three beam groups of A, B and C respectively.

It can be seen from Fig. 7 that as the number of steel wires increased, the total wire stress of the beams L_{A1} to L_{A3} decreased by 31.4%, 13.5%, and 14.9% at the end of the test. With the pre-tension unchanged, when the number of steel wires increased from 2 to 4, the stress loss of the steel wire was significantly reduced. This is because the external load of the beam with four steel wires was increased compared with the beam with two, and the stress of the bamboo-wood composite part was reduced, resulting in a small creep; when the number of steel wires was increased from 4 to 6, the stress loss of the steel wire did not change significantly, because the bearing capacity of the two was relatively close, and the stress of the bamboo-wood composite part was also similar. With the increase of the pre-tension, the total stress values of the steel wires for the beams L_{B1} to L_{B3} decreased by 44.1%, 13.5%, and 17.8%, respectively, and the reasons for such decrease is similar to that of the A-group beams. As the proportion of long-term load applied increased, the total stress value of the steel wires for beams L_{C1} to L_{C3} decreased by 35.8%, 31.4%, and 56.3%, respectively; when the external load was less than 30% of the standard ultimate load, the stress loss of the steel wire had no obvious changes; when the external load was greater than 30%, the steel wire stress changed greatly, and was more sensitive to the external environment.

In order to clarify the change rate of the steel wire stress value, the initial stress of the steel wire was zeroed. Fig. 8 shows the obtained change curve of the relative stress value with time.

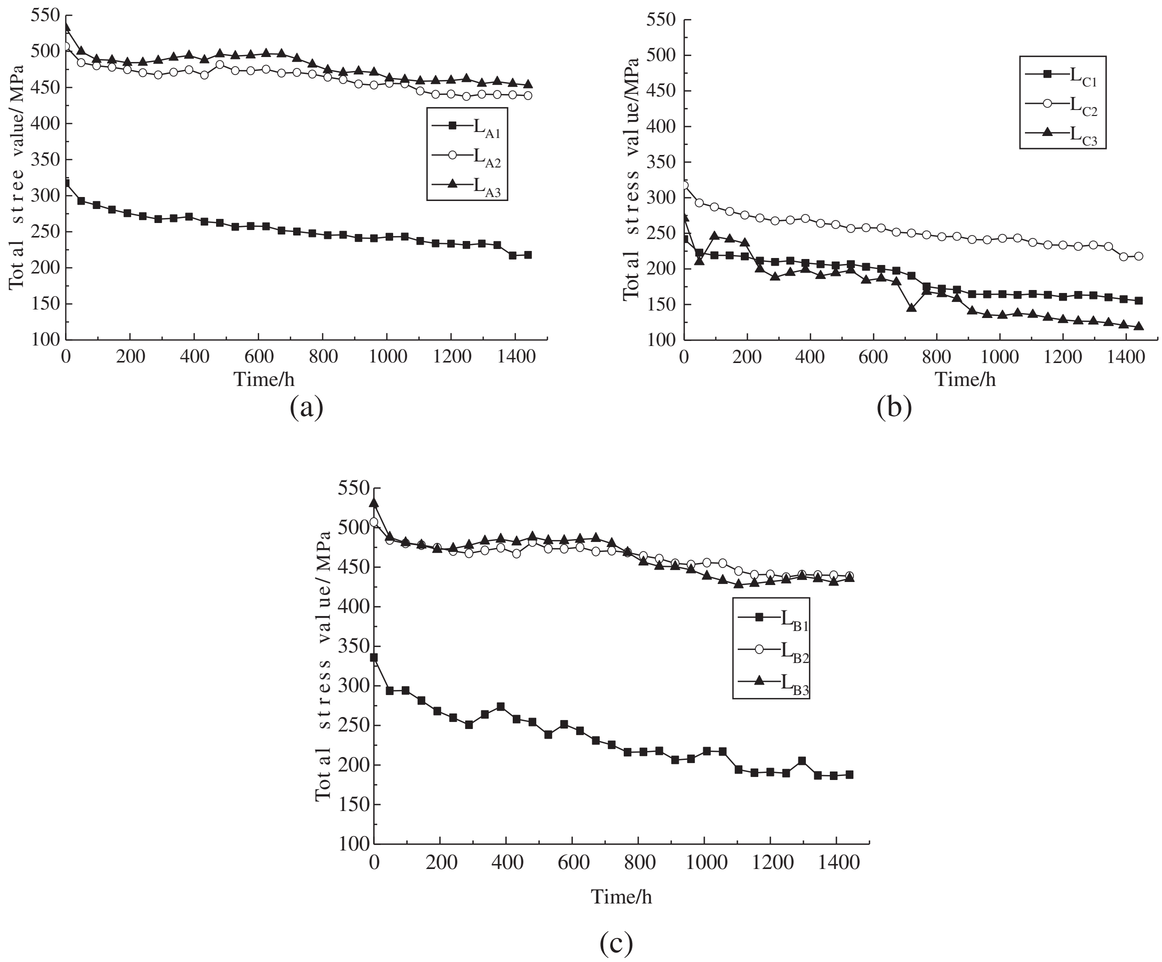

Figure 7: Change curve of total steel wire stress with time. (a) Group A, (b) Group B and (C) Group C

Fig. 8 shows that with the pre-tension and the long-term load unchanged, as the number of steel wires increased, the steel wire stress decreased first and then increased. Overall, the number of pre-stressed wires had no great influence on the falling speed of the total stress value; with the other conditions constant, as the pre-tension increased, the wire stress also decreased first and then increased. At the initial stage of loading, the wire stress of the three beams decreased rapidly, and at the later stage, the falling speed was basically the same, indicating that as the wood starts the plastic deformation, the stress redistribution occurs, and the influence of the pre-tension on the changes of steel wire stress becomes less. When the other conditions were constant, the steel wire stress decreased more rapidly with the long-term load increasing. On the whole, the relative stress variation and the variation rate of the beam L_{C2} and the beam L_{C1} were not much different, which indicates that when the long-term load is greater than 30% of the standard ultimate bearing capacity, it has a significant effect on the total stress of the beam.

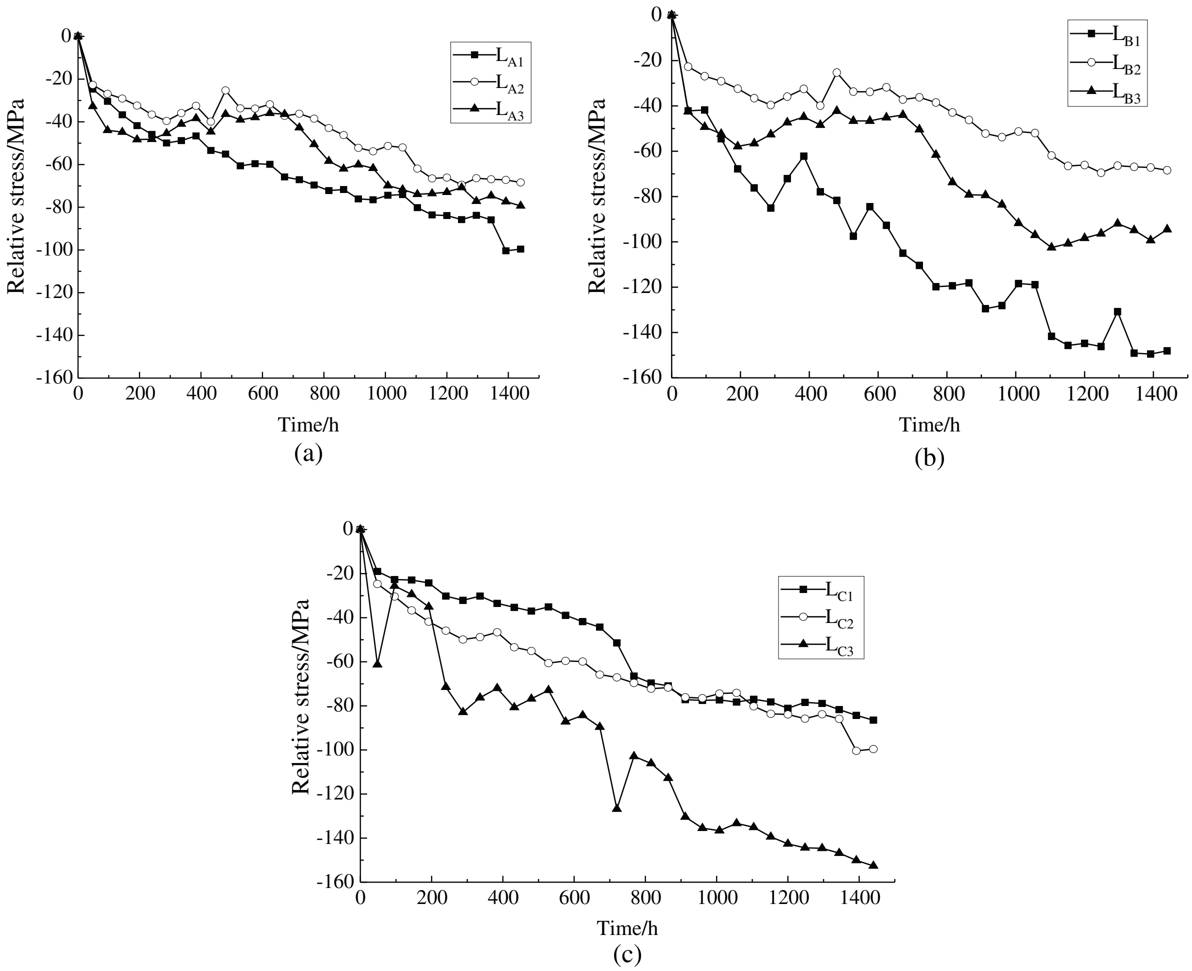

Figure 8: Change curve of relative stress of steel wire with time. (a) Group A, (b) Group B and (c) Group C

3.3 Change Law of Deflection in Beam Midspan

Based on the 60-day observation data of each group of beams, the change curves of the total deflection of the three groups of beams A, B and C with time were obtained. For the convenience of comparison, it is stipulated that "no deformation" of the beam was taken as the origin, and the downward direction of the deflection was positive while he up was negative, as shown in Fig. 9.

Due to the pre-tension applied, the beam had an anti-arch, and then the initial value of the mid-span deflection was negative. After applying the external load, the instantaneous deflection of the beam was short-term deflection; after 60 days of long-term loading, the additional deflection of the beam was long-term deflection; the sum of the two was the total deflection of the beam. The short-term, long-term and total deflection values of the beams Groups A and B are shown in Tab. 2.

Fig. 9 shows that with the other conditions unchanged, when the number of steel wires increased from 2 to 6, the ratio of the long-term deflection on the midspan of the Group A beam to the total deflection was 22.5%, 13.8% and 13.2%, respectively, which indicates that as the number of prestressed wires increased, and the ratio of the long-term deflection on the midspan to the total deflection decreased; however, when the number of pre-stressed steel wires was 4 or more, the effect was not obvious. Besides, with other conditions unchanged, as the pre-tension increased from 1.987 kN to 5.962 kN, the ratio of the long-term deflection on midspan of the B Group to the total deflection was 21.1%, 14.2% and 18.1%, respectively. As the long-term load applied was changed to 3.81 kN, 5.71 kN, 7.61 kN, the ratio of the long-term deflection on the midspan of the C Group to the total deflection was 18.5%, 22.5% and 18.8%, respectively, indicating that the long-term load has no obvious effect on the ratio of long-term deflection in the total deflection.

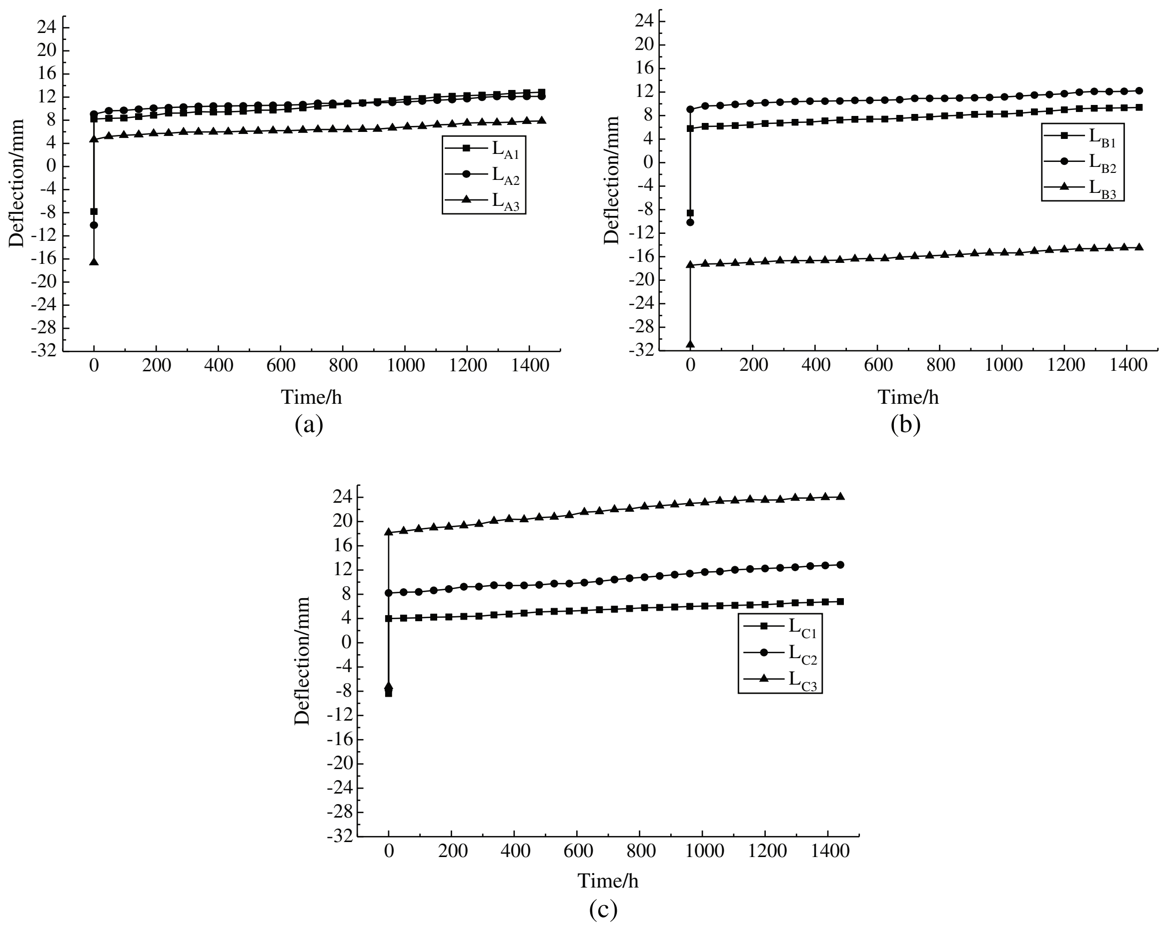

Figure 9: Change curve of total deflection on beam midspan with the time. (a) Group A, (b) Group B and (c) Group C

Taking the deflection of the beam after applying the long-term external load as the origin, the long-term deflection observation data was used to plot the change curve of the long-term deflection on the midspan of each group of beams with time, as shown in Fig. 10.

Fig. 10 shows that under the three test conditions, the long-term deflection of the midspan for the pre-stressed GBWB was increasing, but the speed of the change gradually reduced until it finally stabilized.

For Group A, when the number of prestressed wires increased from 2 to 4, the growth rate of long-term deflection decreased; when the number of steel wires increased from 4 to 6, the growth rate changed little. For Group B, the pre-tension value had no obvious influence on the growth rate of long-term deflection; for Group C, the larger the external load, the faster the growth of long-term deflection.

Table 2: Short-term, long-term, and total deflection of the pre-stressed GBWB

Beam No.	Short-term deflection (mm)	Long-term deflection (mm)	Total deflection (mm)
L_{A1}	16.00	4.65	20.65
L_{A2}	19.22	3.08	22.30
L_{A3}	21.27	3.23	24.50
L_{B1}	14.38	3.85	18.23
L_{B2}	19.22	3.18	22.40
L_{B3}	13.53	3.00	16.53
L_{C1}	12.37	2.80	15.17
L_{C2}	16.00	4.65	20.65
L_{C3}	25.34	5.86	31.20

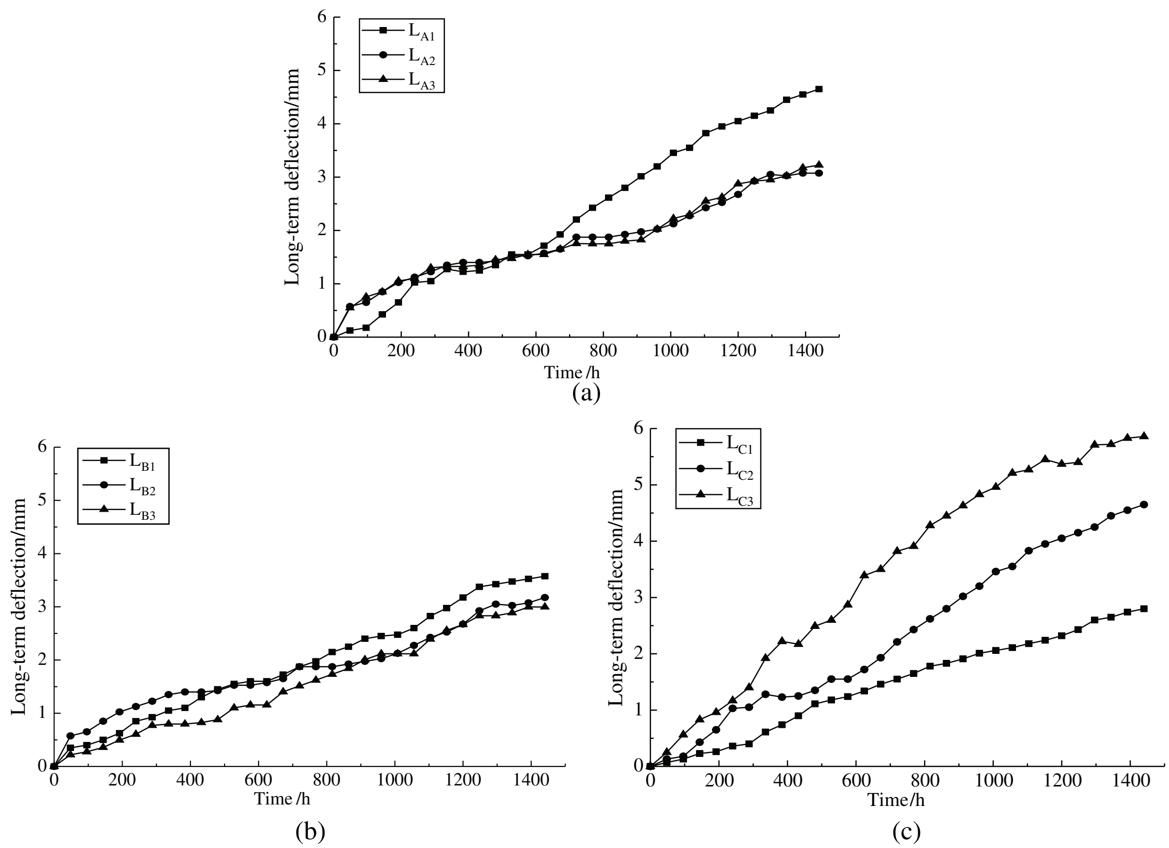

Figure 10: Change curve of the long-term deflection of the beam midspan with time. (a) Group A, (b) Group B and (C) Group C

4 Long-Term Stiffness Analysis Test

4.1 Creep Coefficient θ

In order to better analyse the influence of the pre-stressed GBWB creep on the deflection during long-term loading, this study defines the creep coefficient θ as the ratio of total deflection of the beam during the long-term stable deformation to the instantaneous deflection caused by the external load.

Considering 50-year design life of the general building, data fitting was made for the curve in Fig. 9. Fig. 11 shows the fitting curve and relevant formula of the beam L_{A1}.

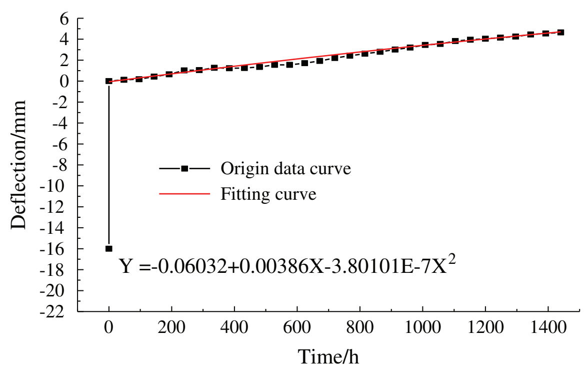

Figure 11: Fitting curve of the total deflection on the L_{A1} beam midspan with time

After fitting analysis, the long-term deflection of beam groups A, B and C is calculated as:

$$y = A + Bt - Ct^2 \tag{9}$$

Among them, the specific values of the coefficients A, B, and C are shown in Tab. 3.

Table 3: Coefficient values for long-term deflection calculation formulas of beams A, B and C

No.	Coefficients		
	A	B	C ($\times 10^{-7}$)
$L_{A1/C2}$	−0.060	0.004	3.801
$L_{A2/B2}$	0.458	0.002	1.577
L_{A3}	0.474	0.002	1.668
L_{B1}	0.115	0.003	2.445
L_{B3}	−0.005	0.003	2.942
L_{C1}	−0.123	0.003	3.575
L_{C3}	−0.171	0.007	16.102

From the above formula, the final long-term deflection of the beam for 50 years was obtained, and then the short-term deflection of the beam was summed up, to derive the final value of the total deflection; the creep coefficient θ was the ratio of the final total deflection to the short-term deflection, as shown in Tab. 4.

It can be seen from Tab. 4 that in the beam Group A, when the number of prestressed wires increased from 2 to 4, the creep coefficient was reduced, and when it is more than 4, the creep coefficient was basically unchanged; for the B beam group, when the pre-tension increased from 1.987 kN to 3.975 kN, the prestressing value had little effect on the creep coefficient; in the C-Group, the creep coefficient increased first and then decreased with the increasing of the long-term load value.

According to the test results, it's recommended to take the value of creep coefficient θ in the range of 1.2–1.8. Meanwhile, compared with the creep coefficient of the glulam beam studied in the earlier stage, the creep coefficient of the pre-stressed GBWB was significantly smaller.

Table 4: Long-term relative deflection limit and creep coefficient of the pre-stressed GBWB

Item	Total deflection (mm)	Variation of instantaneous deflection (mm)	Limit value of long-term deflection (mm)	Creep coefficient θ
$L_{A1/C2}$	22.49	12.75	9.74	1.76
$L_{A2/B2}$	26.73	19.22	7.51	1.39
L_{A3}	28.74	21.27	7.47	1.35
L_{B1}	22.56	14.38	8.19	1.57
L_{B3}	19.18	13.53	5.65	1.42
L_{C1}	16.72	12.37	4.35	1.35
L_{C3}	31.93	25.34	6.59	1.26

4.2 Calculation Formula of Long-Term Stiffness B

In order to facilitate the derivation of formulas, the prestressed glued bamboo and wood beam for this test is simplified as shown in Fig. 12.

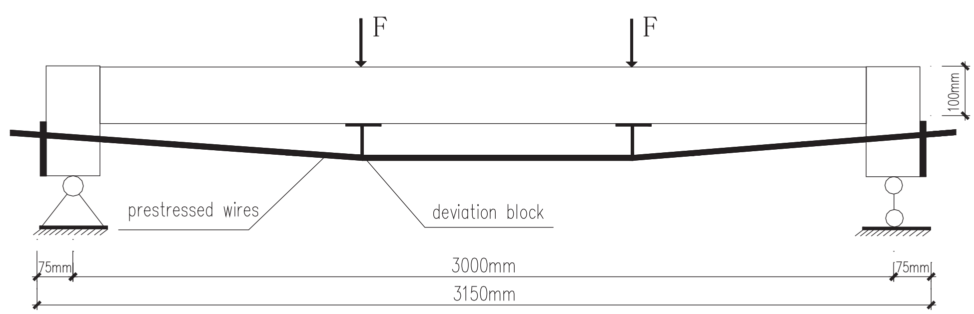

Figure 12: The schematic diagram of the prestressed glued bamboo and wood beam

4.2.1 Deflection Without Consideration of Prestressing Effects

According to the algorithm of "deflection and rotation angle of beams under simple loads" in material mechanics, when a concentrated force acts on a simply supported beam, the deflection calculation formula is shown in the formula (10):

$$w_x = \frac{pbx}{6EIl}(l^2 - x^2 - b^2), 0 \leq x \leq a \tag{10}$$

$$\frac{pb}{6EIl}[\frac{b}{l}(x-a)^2 + (l-b)x - x^3], a \leq x \leq l$$

This test uses three-point loading. The loading diagram is shown in Fig. 14.

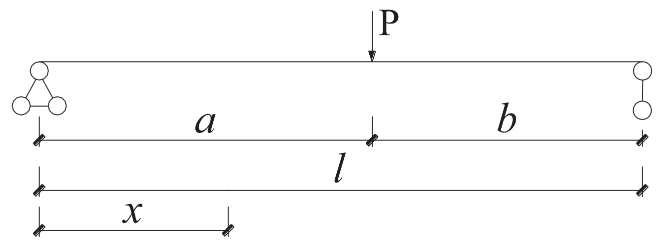

Figure 13: The schematic diagram of the concentrated force

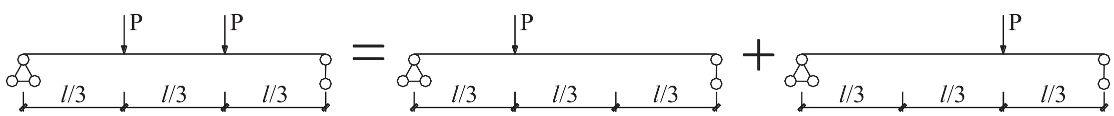

Figure 14: The loading diagram

It can be seen that the mid-span deflection is equal to twice the deflection of the beam when the external load alone acts on the three dividing point on one side of the beam. The formula (11) is:

$$w_{1/2} = w_{left} + w_{right} = 2w_{left} \tag{11}$$

When $x = l/2$, $p = F/2$, and $b = l/3$, substituting them into the formula (10) gives:

$$w_{right} = \frac{23}{36} \times \frac{Fl}{72EI} l^2 \tag{12}$$

$$w_{1/2} = 2w_{right} = 23Fl^3/(1296E_m I_m) \tag{13}$$

where E_{m} is the elastic modulus of the pure bending section of the prestressed glued bamboo and wood beam; I_{m} is the second moment of area of the pure bending section of the prestressed glued bamboo and wood beam.

The mid-span moment M in the test is:

$$M = Fl/(2 \times 3) = Fl/6 \tag{14}$$

4.2.2 Deflection with Consideration of Prestressing Effects

Before the test beam is loaded, the prestress is applied to the glued bamboo and wood beam. However, the prestress will cause an inverted arch of the beam. Therefore, when the deflection of the prestressed glued bamboo and wood beam in this test is calculated, the inverted arch value caused by the prestress should be subtracted.

Before the prestressed glued bamboo and wood beam is loaded in this test, the beam needs to be prestressed by a prestressing control device placed at the three dividing point of the beam, as shown in Fig. 15.

Before the formal test, it is necessary to determine the reasonable range of the prestress value based on the tensile strength of the fiber at the top of the glued bamboo and wood beam after applying the prestress. Assuming that the beam span is l. Before the prestress is applied, the distance between the mid-span wire and the bottom of the glued bamboo and wood beam is h_1. After the prestress is applied, the increment is h_2. The prestressed glued bamboo and wood beam in this test is simplified, as shown in Fig. 16.

For a two-point tension string, the length of the prestressed wire before the prestress is applied can be obtained:

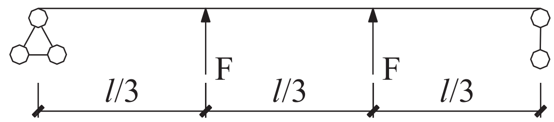

Figure 15: The schematic diagram of prestressing points

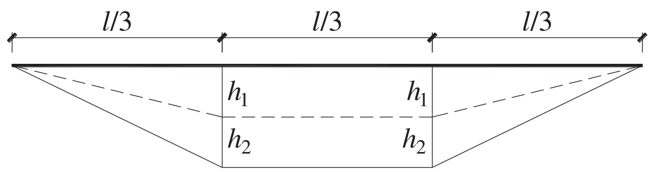

Figure 16: Overall calculation sketch of the pre-stressed GBWB

$$l_1 = 2\sqrt{(\frac{l}{3})^2 + h_1^2} + \frac{l}{3} \tag{15}$$

After the prestress is applied, the length of the prestressed wire is:

$$l_2 = 2\sqrt{(\frac{l}{3})^2 + (h_1 + h_2)^2} + \frac{l}{3} \tag{16}$$

The elongation of the prestressed wire during this process is:

$$\Delta l_p = l_1 - l_2 = 2[\sqrt{(\frac{l}{3})^2 + (h_1 + h_2)^2} - \sqrt{(\frac{l}{3})^2 + h_1^2}] \tag{17}$$

After the prestress is applied, the strain value of the prestressed wire can be obtained: $\varepsilon_{\rm p} = \Delta l_{\rm p}/l_1$. At this time, the stress value of the prestressed wire is:

$$\sigma_p = \varepsilon_p E_p = E_p(\frac{\sqrt{\left(\frac{1}{3}\right)2 + (h_1 + h_2)^2} + \frac{1}{3}}{\sqrt{(\frac{1}{3})^2 + h_1^2} + \frac{l}{3}} - 1) \tag{18}$$

The axial force of the bolt rod is:

$$F_s = \frac{\sigma_p A_p (h_1 + h_2)}{\sqrt{\left(\frac{l}{3}\right)^2 + (h_1 + h_2)^2}} = E_p A_p (h_1 + h_2)[\frac{1 - \frac{\sqrt{(\frac{l}{3})^2 + h_1^2}}{\sqrt{(\frac{l}{3})^2 + (h_1 + h_2)^2}}}{\sqrt{(\frac{l}{3})^2 + h_1^2} + \frac{1}{3}}] \tag{19}$$

As shown in Fig. 15, the glued bamboo and wood beam is isolated to analyze its force, and the force on the bolt rod is concentrated in the beam span. At this time, the arch value in the beam span caused by $F_{\rm s}$ is:

$$f = \frac{F_s l^3}{48E_m I_m} = \frac{E_p A_p (h_1 + h_2) l^3}{48E_m I_m} \left[\frac{1 - \frac{\sqrt{(\frac{l}{3})^2 + h_1^2}}{\sqrt{(\frac{l}{3})^2 + (h_1 + h_2)^2}}}{\sqrt{(\frac{l}{3})^2 + h_1^2} + \frac{1}{3}} \right] \tag{20}$$

where E_p is the elastic modulus of the prestressed wire; A_p is the cross-sectional area of the prestressed wire.

The total deformation of the beam, that is, the deflection of the beam, should be the result of the joint action of external loads and prestress. Therefore, when the total value of the external load (jack) is F, the total deformation of the beam is:

$$\Delta = w_{1/2} - f \tag{21}$$

From formulas (13), (20) and (21), it can be known that to determine the deflection of the beam, the stiffness of the beam must be determined first. According to the test data, the long-term stiffness and short-term stiffness of the prestressed glued bamboo and wood beam are different. To calculate the long-term deflection of the prestressed glued bamboo and wood beam, its long-term stiffness should be used.

Because there is not any method to calculate the long-term creep in the *Code for Design of Timber Strucutre* (GB50005-2017) [35]. Drawing on the relevant provisions that propose formulas to calculate long-term stiffness in the *Code for Design of Concrete Structures* (GB50010-2010) [36], test results and engineering experience,one formula was proposed to calculate the stiffness of the pre-stressed GBWB after long-term loading. The calculation sketch is shown in Fig. 16, where the span of the beam is L, the distance between the steel wire at the mid-span position and the bottom of the beam before prestressing is h_1, and the distance between the steel wire and the bottom of the beam after prestressing is increased by h_2.

$$B = \frac{M_k}{[M_q \times (\theta - 1) + M_k]} \times B_s \tag{22}$$

where:

B-the stiffness of the bent member considering the long-term effect of the load;

B_s-the short-term stiffness of the prestressed bend members calculated according to the standard combination;

θ-the creep coefficient of the pre-stressed GBWB considering the long-term load effect, taking 1.2–1.8;

M_k-the bending moment calculated according to the standard combination of loads, taking the maximum bending moment value in the calculation section;

M_q-the bending moment calculated by the quasi-permanent combination of loads, taking the maximum bending moment value in the calculation section.

5 Conclusions

(1) When the number of steel wires increased from 2 to 4, the stress loss of the steel wire was significantly reduced, the ratio of the long-term deflection of the beam midspan to the total deflection decreased, and the growth rate of the long-term deflection slowed down; When the number was up to six, the above parameters did not change much;

(2) When the pre-tension increased from 1.987 kN to 3.975 kN, the total stress value of the steel wire decreased significantly, the steel wire stress decreased rapidly, and the ratio of the long-term deflection of the beam midspan to the total deflection was also reduced; When it increases from 3.975 kN to 5.962 kN, the above parameters did not change much;

(3) When the external load was less than 30% of the standard ultimate load, the stress loss and the falling speed of the steel wire stress decreased slowly; when the external load was greater than 30% of the standard value, the stress of the steel wire changed greatly, being more sensitive to the external environment, and the steel wire stress declined more rapidly. In addition, the long-term load size had little effect on the ratio of long-term deflection to total deflection, but the larger the external load, the faster the growth of long-term deflection;

(4) According to the power law model, the long-term deflection of the beam for 50 years, and the creep coefficient of the prestressed beam were obtained, that is, in the case of normal number of prestressed wires and the normal pre-tension value, it is recommended to take the value of the creep coefficient θ in the range of 1.2–1.8. After that, combined with the relevant specifications, the long-term stiffness calculation formula of the prestressed beam was given.

Funding Statement: In the process, this project was supported by the Fundamental Research Funds for the Central Universities (2572017DB02), the natural science foundation of heilongjiang province (LH2019E005) and Harbin science and technology innovation talent fund project (2017RAQXJ086).

Conflicts of Interest: The authors declare that they have no conflicts of interest to report regarding the present study.

References

1. Sui, Y. K., Chang, J. Y., Ye, H. L. (2009). Numerical simulation of semi-rigid element in timber structure based on finite element method. *Computational Structural Engineering, 6,* 643–652.
2. Muhtar, M., Dewi, S. M., Munawir, A. W. (2019). Bridge structure from bamboo reinforced concrete frame. *Proceedings of the 11th Asia Pacific Transportation and the Environment Conference*.
3. Wang, Y. Y., Yin, H. (2014). Analysis on significance of bamboo products based on sustainable development. *Advanced Materials Research, 1010–1012,* 1944–1948. DOI 10.4028/www.scientific.net/AMR.1010-1012.1944.
4. Singh, S. R., Singh, R., Kalia, S., Dalal, S., Dhawan, A. K. et al. (2013). Limitations, progress and prospects of application of biotechnological tools in improvement of bamboo—a plant with extraordinary qualities. *Physiology and Molecular Biology of Plants, 19(1),* 21–41. DOI 10.1007/s12298-012-0147-1.
5. Zhang, A. H. (2009). The ecological prospects of Chinese bamboo design. *Proceedings of the 3rd International Conference on Mechanical Engineering and Mechanics, 2,* 1021–1027.
6. Yue, K., Wang, L., Xia, J., Zhang, Y. L., Chen, Z. J. et al. (2019). Structural assessment of laminated wood veneer/plastic sheet composites used as building material. *Wood and Fiber Science, 51(3)*.
7. Fang, H., Sun, H. M., Liu, W. Q., Wang, L., Bai, Y. et al. (2015). Mechanical performance of innovative GFRP-bamboo-wood sandwich beams: experimental and modelling investigation. *Composites Part B: Engineering, 79,* 182–196. DOI 10.1016/j.compositesb.2015.04.035.
8. Xu, Q. F., Chen, X., Chen, J. F., Kent, A. H., Chen, L. Z. et al. (2019). Seismic strengthening of masonry walls using bamboo components. *Science Citation Index Expanded, 22,* 2982–2997.
9. Moroz, J. G., Lissel, S. L., Hagel, M. D. (2014). Performance of bamboo reinforced concrete masonry shear walls. *Construction and Building Materials, 61,* 125–137. DOI 10.1016/j.conbuildmat.2014.02.006.
10. Song, J., Surjadi, J. U., Hu, D. Y., Lu, Y. (2017). Fatigue characterization of structural bamboo materials under flexural bending. *International Journal of Fatigue, 100,* 126–135. DOI 10.1016/j.ijfatigue.2017.03.016.
11. Chen, F. M., Jiang, Z. H., Wang, G., Li, H. D., Simth, L. M. et al. (2016). The bending properties of bamboo bundle laminated veneer lumber (BLVL) double beams. *Construction and Building Materials, 119,* 145–151. DOI 10.1016/j.conbuildmat.2016.03.114.

12. Huang, D. S., Zhou, A. P., Bian, Y. L. (2013). Experimental and analytical study on the nonlinear bending of parallel strand bamboo beams. *Construction and Building Materials, 44,* 585–592. DOI 10.1016/j.conbuildmat.2013.03.088.
13. Li, H. T., Wu, G., Zhang, Q. S., Deeks, A. J., Su, J. W. (2016). Ultimate bending capacity evaluation of laminated bamboo lumber beams. *Construction and Building Materials, 160,* 365–375. DOI 10.1016/j.conbuildmat.2017.11.058.
14. Li, H. T., Zhang, Q. S., Huang, D. S., Deeks, A. J. (2013). Compressive performance of laminated bamboo. *Composites Part B: Engineering, 54,* 319–328. DOI 10.1016/j.compositesb.2013.05.035.
15. Li, H. T., Xiong, X. H., Zhang, Q. S., Shao, M., Xiong, X. J. et al. (2016). Bending performance of laminated bamboo. *World Conference on Timber Engineering proceeding. WCTE 2016 e-book, Vienna*, *8,* 932–940.
16. Guo, N., Chen, H. H., Zhang, P. Y., Zuo, H. L. (2016). The research of parallel to the grain compression performance test of laminated glued bamboo-wood composites. *Technicalgazetee, 23(1),* 129–135.
17. Sun, Y. H., Jiang, Z. H., Liu, H. R., Sun, Z. J. F., Chang, H. (2019). The bending properties of bamboo strand board I-beams. *Journal of Wood Science, 65(1),* 1–10. DOI 10.1186/s10086-019-1828-y.
18. Zhao, J. B., Meng, Z. X., Jin, Z., Chen, D., Wu, Y. S. et al. (2019). Bending properties of bamboo scrimber with holes in different sizes and positions. *Construction and Building Materials, 200,* 209–217. DOI 10.1016/j.conbuildmat.2018.12.076.
19. Zhong, Y., Wu, G. F., Ren, H. Q., Jiang, Z. H. (2017). Bending properties evaluation of newly designed reinforced bamboo scrimber composite beams. *Construction and Building Materials, 143,* 61–70. DOI 10.1016/j.conbuildmat.2017.03.052.
20. Guo, N., Wang, Y. J., Zuo, H. L. (2017). Study of short-term flexural behavior for glue-bamboo and lumber beams under different pre-stressed states. *Civil Engineering Journal, 26(2),* 128–142.
21. Yang, H. F., Liu, W. Q., Lu, W. D., Zhu, S. J., Geng, Q. F. (2016). Flexural behavior of FRP and steel reinforced glulam beams: experimental and theoretical evaluation. *Construction and Building Materials, 106,* 550–563. DOI 10.1016/j.conbuildmat.2015.12.135.
22. Yang, H. F., Ju, D. D., Liu, W. Q., Lu, W. D. (2016). Prestressed glulam beams reinforced with CFRP bars. *Construction and Building Materials, 109,* 73–83. DOI 10.1016/j.conbuildmat.2016.02.008.
23. Zuo, H., Hou, J., Yu, Z., Guo, N. (2015). The bending performance experimental study on material selection of prestressed high strength glue-lumber beam. *Chemical Engineering Transactions, 46,* 109–114.
24. Guan, W. Z., Rodd., D. P., Pope, J. D. (2005). Study of glulam beams pre-stressed with pultruded GRP. *Computers & Structures, 83(28–30),* 2476–2487. DOI 10.1016/j.compstruc.2005.03.021.
25. Gottron, J., Kent, A. H., Xu, Q. F. (2014). Creep behaviour of bamboo. *Construction and Building Materials, 66,* 79–88. DOI 10.1016/j.conbuildmat.2014.05.024.
26. MaSheldon, Q. X. X., Fei, S. G. W. B. H., Jiang, Z. H. (2018). Long creep-recovery behavior of bamboo-based products. *Journal of Wood Science, 64(2),* 119–125l. DOI 10.1007/s10086-017-1683-7.
27. Ngudiyono, N., Suhendro, B., Awaludin, A., Triwiyono, A. (2019). Review of creep modelling for predicting of long-term behavior of glued-laminated bamboo structures. *International Conference on Sustainable Civil Engineering Structures and Construction Materials,* 258, Royal Ambarrukmo Yogyakarta.
28. Li, L. (2012). *Research on creep property of glubam and modern bamboo composite structure*. Changsha, Hunan University.
29. NurYazdani, P. E., Johnson, E., Duwadi, S. (2004). Creep effect in structural composite lumber for bridge applications. *Journal of Bridge Engineering, 9(1),* 87–94. DOI 10.1061/(ASCE)1084-0702(2004)9:1(87).
30. Xiao, Y., Li, L., Yang, R. Z., Shan, B., She, L. Y. (2013). Experimental study on creep and loading property of laminated bamboo bridge. *Building Structure, 43(18),* 86–91.
31. LY/T 1975-2011 (2011). Standard for evaluation of duration of load creep effects of wood and wood-based products. Beijin,Standards Press of China.
32. Pan, J. L., Zhu, E. C. (2009). *Design principle of wood structure,* pp. 2–4. Beijin, China Architecture & Building Press.

33. GB50009-2012 (2012). *National standard of the people's Republic of China: load code for the design of building structures*. Beijing: China Architecture & Building Press.
34. Yang, Y. W. (2015). *The study on flexural performance of prestressed glulam beams string structure based on the creep behavior*. Harbin, Northeast Forestry University.
35. GB50005-2017 (2017). *National standard of the people's Republic of China: the code for design of timber structure*. Beijing: China Architecture & Building Press.
36. GB50010-2010 (2010). *National standard of the people's Republic of China: the code for design of concrete structures*. Beijing: China Architecture & Building Press.